ChemPubSoc Europe

DOI: 10.1002/cphc.201700843

CHEMPHYSCHEM Articles

Interaction of Ester-Functionalized Ionic Liquids with Atomically-Defined Cobalt Oxides Surfaces: Adsorption, Reaction and Thermal Stability

Tao Xu,[a] Tobias Waehler,[a] Julia Vecchietti,[b] Adrian Bonivardi,[b] Tanja Bauer,[a] Johannes Schwegler,[c] Peter S. Schulz,[c] Peter Wasserscheid,[c] and Joerg Libuda*[a, d]

Hybrid materials consisting of ionic liquid (ILs) films on supported oxides hold a great potential for applications in electronic and energy materials. In this work, we have performed surface science model studies scrutinizing the interaction of ester-functionalized ILs with atomically defined Co_3O_4(111) and CoO(100) surfaces. Both supports are prepared under ultra-high vacuum (UHV) conditions in form of thin films on Ir(100) single crystals. Subsequently, thin films of three ILs, 3-butyl-1-methyl imidazolium bis(trifluoromethyl-sulfonyl) imide ([BMIM][NTf_2]), 3-(4-methoxyl-4-oxobutyl)-1-methylimidazolium bis(trifluoromethyl-sulfonyl) imide ([MBMIM][NTf_2]), and 3-(4-isopropoxy-4-oxobutyl)-1-methylimidazolium bis(trifluoromethyl-sulfonyl) imide ([IPBMIM][NTf_2]), were deposited on these surfaces by physical vapor deposition (PVD). Time-resolved and temperature-programmed infrared reflection absorption spectroscopy (TR-IRAS, TP-IRAS) were applied to monitor in situ the adsorption, film growth, and thermally induced desorption. By TP-IRAS, we determined the multilayer desorption temperature of [BMIM][NTf_2] (360 ± 5 K), [MBMIM][NTf_2] (380 K) and [IPBMIM][NTf_2] (380 K). Upon deposition below the multilayer desorption temperature, all three ILs physisorb on both cobalt oxide surfaces. However, strong orientation effects are observed in the first monolayer, where the $[NTf_2]^-$ ion interacts with the surface through the SO_2 groups and the CF_3 groups point towards the vacuum. For the two functionalized ILs, the $[MBMIM]^+$ and $[IPBMIM]^+$ interact with the surface Co^{2+} ions of both surfaces via the CO group of their ester function. A very different behavior is found, if the ILs are deposited above the multilayer desorption temperature (400 K). While for [BMIM][NTf_2] and [MBMIM][NTf_2] a molecularly adsorbed monolayer film is formed, [IPBMIM][NTf_2] undergoes a chemical transformation on the CoO(100) surface. Here, the ester group is cleaved and the cation is chemically linked to the surface by formation of a surface carboxylate. The IL-derived species in the monolayer desorb at temperatures around 500 to 550 K.

1. Introduction

Ionic liquids (ILs) are, by definition, salts which are liquid at temperatures below 100 °C.[1] An interesting feature of this class of compounds is their low vapor pressure, which enables the preparation of stable liquid coatings in presence of vacuum. This extraordinary property along with the tuneability of other physiochemical parameters like solubility, solvation, viscosity, density or thermal stability led to various applications of ILs in catalysis,[2] energy technology,[3] or molecular electronics,[4] just to name a few.[5] In many of these applications, performance relies on the transport of electrons, protons or chemical species across the IL/solid interface and, consequently, the nature of this interface plays a crucial role for the overall performance of the corresponding devices.[5b] However, our fundamental understanding of such interfaces is still quite limited and our capabilities to engineer such interfaces are in their infancy. At the microscopic level, major challenges arise from the nature of ILs being "non-classical" electrolytes and the intrinsic chemical complexity of liquid/solid interfaces where specific interactions and, in some cases, even specific interface reaction may occur.[2a,6] Thus, a better understanding of chemical interactions and reactivity at the IL/solid interface are urgently required to tailor interface functionality for specific applications.

A particularly challenging case is that of IL/oxide interfaces which play an important role in catalysis,[2] solar cells,[7] and organic electronics.[8] A growing number of researches on the IL/oxide or IL/metal interface has been reported.[9] In most of these cases, the ILs are physisorbed on the oxide surface via

[a] T. Xu, T. Waehler, T. Bauer, Prof. Dr. J. Libuda
Lehrstuhl für Physikalische Chemie II
Friedrich-Alexander-Universität Erlangen-Nürnberg
Egerlandstraße 3, 91058 Erlangen (Germany)
Fax: +49 9131 8527308
E-mail: joerg.libuda@fau.de

[b] Dr. J. Vecchietti, Prof. Dr. A. Bonivardi
Instituto de Desarrollo Tecnológico para la Industria Química (INTEC)
UNL-CONICET, Güemes 3450, 3000 Santa Fe (Argentina)

[c] J. Schwegler, Dr. P. S. Schulz, Prof. Dr. P. Wasserscheid
Lehrstuhl für Chemische Reaktionstechnik
Friedrich-Alexander-Universität Erlangen-Nürnberg
Egerlandstrasse 3, 91058 Erlangen (Germany)

[d] Prof. Dr. J. Libuda
Erlangen Catalysis Resource Center and
Interdisciplinary Center for Interface Controlled Processes
Friedrich-Alexander-Universität Erlangen-Nürnberg
91058 Erlangen (Germany)

Supporting Information and the ORCID identification number(s) for the author(s) of this article can be found under: https://doi.org/10.1002/cphc.201700843.

van-der-Waals or electrostatic interactions while some layering effect of ILs are commonly seen at the interface. On another hand, reports on the chemical interaction of IL with the oxide surface via specific functional groups are scarce. The most well-established method is functionalization via silanol chemistry.[10] One drawback of this method is, however, that silicon oxide groups are introduced into the interface, which is less desired if the electronic properties of the interface are critical. In our previous studies, we showed that these different interactions are indeed observed, depending on the nature of the oxide surface, the IL and the experimental conditions. For instance, we showed that [BMIM][NTf_2] adsorbs molecularly on alumina films, but with a characteristic orientation adopted by the anion.[11] In sharp contrast, interfacial reactions were observed for [HMIM][NTf_2] (3-hexyl-1-methyl imidazolium bis(trifluoromethyl-sulfonyl) imide) on ceria, depending on the stoichiometry of the surface. On oxygen terminated CeO(111), we observed a chemical transformation of the cation, initiated by deprotonation and subsequent transalkylation.[12] Such reactions may be used to functionalize oxide surfaces to form stable and well-defined IL/oxide interfaces. Towards this aim, however, general methods that are applicable to a broad range of ILs and oxides would be most desirable.

An alternative approach to functionalize oxide surfaces makes use of specific anchor groups, such as carboxylic acids,[13] phosphonic acids[14] or others.[15] The introduction of anchor groups is a well-proven method to link organic films to oxides, however, the concept has not been applied to ILs yet. One concern is, for instance, that the anchor groups could affect the thermal and electrochemical stability of the IL.[16] Fundamental investigations on well-defined oxide surfaces are therefore needed to explore scope and limitations of this concept to tune IL-oxide interactions via functionalization of the IL.

In this study, we investigate the interaction of ester-functionalized ILs on atomically defined cobalt oxide surfaces. The ester group was chosen instead of a free carboxylic acid as it leads to a higher volatility of the respective functionalized IL, a fact that eases the preparation of thin IL films by physical vapor deposition (PVD). This allows us to coat the oxide surface with an ultraclean IL film in a well-controlled fashion.[17,6a] We performed all experiments under ultrahigh vacuum (UHV) conditions, taking advantage of the extremely low vapor pressure of ILs.[6] By using well-defined surfaces and UHV conditions, we identify the molecular interactions at the IL/oxide interface and the chemical transformation upon anchoring of the functionalized ILs. Co_3O_4(111) and CoO(100) model surfaces were chosen because of the wide range of very interesting properties of cobalt oxides in catalysis,[18] electro-catalysis,[19] and as magnetic materials.[20] In previous studies we investigated the functionalization of these surfaces by carboxylic acids.[21]

In this work, we applied IRAS to follow the adsorption of [BMIM][NTf_2], [MBMIM][NTf_2] and [IPBMIM][NTf_2] (Scheme 1) on two atomically-defined cobalt oxide surfaces, Co_3O_4(111) and CoO(100) (Scheme 2). Surface science studies of such functionalized ILs on reactive oxides are still extremely scarce.[12] The

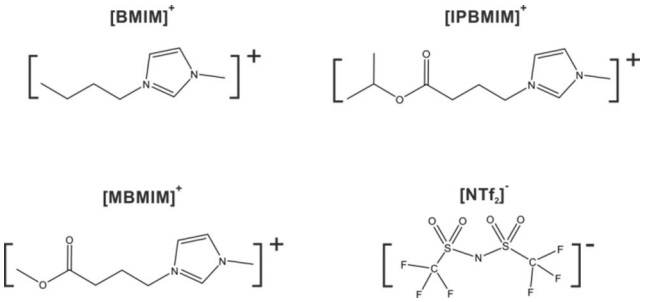

Scheme 1. Molecular structure of the ILs and abbreviations used in this work.

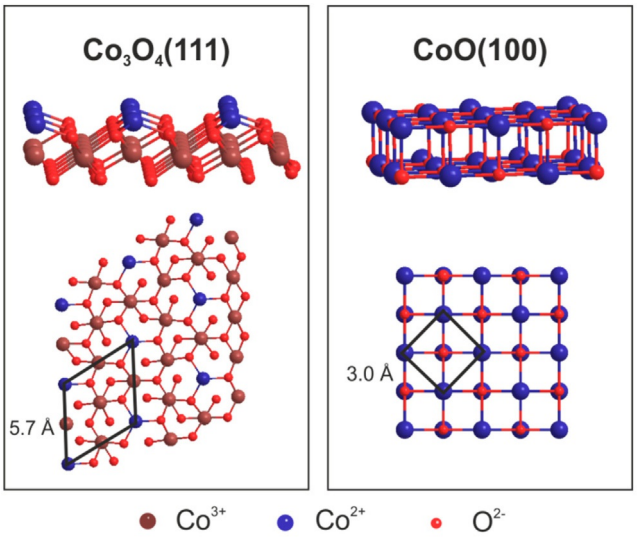

Scheme 2. Structure model of the Co_3O_4(111) and CoO(100) surfaces. The Co_3O_4(111) surface is terminated by Co^{2+} ion with the O^{2-} and Co^{3+} lying in the second and third layer. The Co^{2+}–Co^{2+} distance is 5.7 Å. The CoO(100) surface is terminated both by Co^{2+} and O^{2-} with a Co^{2+}–Co^{2+} distance of about 3.0 Å (see the review[26] by Heinz and Hammer etc. for details).

cobalt oxide films provide an ideal test system to explore the interaction mechanisms of ILs with atomically defined oxide surfaces of known structure. First results from this research were previously published in a form of a short communication.[22] Here, we present a more comprehensive description of the results.

Experimental Section

IRAS under Isothermal Conditions

All sample preparation and IRAS measurements were performed in an UHV chamber (base pressure 2.0×10^{-10} mbar). The details about the set-up have been described elsewhere.[23] The IR spectra were acquired with a Fourier-transform infrared (FTIR) spectrometer (Bruker Vertex 80v) connected to the measuring chamber via differentially pumped KBr windows. All IR spectra were recorded with a resolution of 2 cm^{-1}. Prior to the deposition, a reference spectrum was recorded on the clean surface, typically with an acquisition time of 5 min. For the isothermal adsorption measurements, the sample was kept at a stable temperature by balancing

cooling with liquid nitrogen and heating with radiation and/or electron bombardment from backside. During deposition of the ILs, the IR spectra were acquired continuously with an acquisition time of 60 s per spectrum.

Temperature-programmed IRAS

For the TP-IRAS measurements the sample was heated with a constant rate of 2 K min^{-1} using a temperature controller. Simultaneously, IR spectra were recorded continuously with an acquisition time of 60 seconds per spectrum.

Preparation of Co_3O_4(111)/Ir(100)

Co3O4(111) thin films were prepared by reactive deposition of Co in O_2 atmosphere, following a procedure developed by Heinz, Hammer and co-workers.[24] The procedure was slightly modified regarding the O_2 partial pressure and annealing temperatures. First, the Ir(100) single crystal (MaTeck) was cleaned by cycles of Ar^+ sputtering (1.8 keV, 300 K, 1 hour; Ar, Linde, 6.0) and annealing (1100 °C, 3 min) until a clear 5×1 LEED pattern (room temperature) of the Ir(100)-(5×1) reconstructed surface appeared. Secondly, the Ir(100)-(5×1) surface was heated to 1000 °C in 8×10^{-8} mbar O_2 (Linde, 5.0) for 3 min and, subsequently, cooled down to room temperature in O_2 atmosphere. This led to the formation of an Ir(100)-(2×1)O reconstructed surface showing a clear 2×1 LEED pattern. After a flashing to 300 °C, Co was evaporated onto the cooled surface (at sample temperatures below 0 °C) using a commercial electron beam evaporator (Focus EFM3, 2 mm Co rod, Alfa Aesar 99,995%, or Goodfellow 99.99%) in 5.0×10^{-6} mbar O_2 for 30 min. At the Co deposition rate used in this work, this yields a Co_3O_4 film with a thickness of approximately 6 nm. After the growth, the film was annealed in O_2 (1.0×10^{-6} mbar) to 250 °C for 2 min and then in UHV to 480 °C for 5 min. The film was checked qualitatively by comparing the LEED I–V curves with literature.[24]

Preparation of CoO(100)/Ir(100)

The CoO film was prepared using a procedure developed by Heinz, Hammer and co-workers.[25] A metastable Ir(100)-(1×1) reconstructed surface was prepared in the first step, starting from the clean Ir(100)-(5×1) surface and preparing the Ir(100)-(2×1)O surface (see procedure above). Subsequently, the sample was heated to 275 °C in 1×10^{-7} mbar H_2 (Linde, 5.3) for 1 min and, thereafter, in UHV to 275 °C for 1 min before cooling down to room temperature again. This procedure yielded the Ir(100)-(1×1) surface as identified by LEED. Subsequently, metallic Co was deposited onto the surface (50 °C) at a rate of 1.5 MLE min^{-1} (1 MLE = 1.36×10^{15} atoms cm^{-2}) for 5 min. After growth of the Co buffer layer, the sample was cooled to temperatures below −50 °C. Then Co was deposited at a rate of 1.5 MLE min^{-1} in 6×10^{-7} mbar O_2 for 3 min. Subsequently, the film was annealed to 100 °C for 1 min yielding an ordered CoO(100) structure. For the preparation of thicker and better ordered CoO(100) films, a second reactive deposition step with Co atoms in O_2 (rate: 1.5 MLE min^{-1}, deposition time: 30 min) was performed while keeping the sample at low temperature (< −50 °C). Subsequently, the CoO(100) film was annealed to 800 °C for 5 min in UHV. After this treatment, the as-prepared CoO(100) thin film showed a sharp 1×1 pattern in LEED.

PVD of ILs

All ILs were deposited from ceramic crucibles using home-build resistively heated evaporators.[11] The evaporators were separated from the measuring chamber by a gate valve and before deposition pumped by a separate high vacuum system. Prior to each deposition, the ILs were heated (110 °C for [MBMIM][NTf_2], 120 °C for [IPBMIM][NTf_2] and 100 °C for [BMIM][NTf_2]) before opening the gate valve to the measuring chamber to prevent contamination.

Synthesis of ILs

All ILs were specially synthesized in very high purity for the purpose of this study. All details on the synthesis and characterization are provided in the Supporting Information.

2. Results and Discussion

Three different ILs were used in the present study, [MBMIM][NTf_2], [IPBMIM][NTf_2] and [BMIM][NTf_2]. The structure of the anions and cations are shown in Scheme 1. All three ILs have the same anion, namely [NTf_2]$^-$, and differ in the side-chain functionalization of their imidazolium ions. Whereas [MBMIM]$^+$ contains a methyl ester group in the side chain, the [IPBMIM][NTf_2] carries a isopropyl ester side chain.

The ordered Co_3O_4(111) and CoO(100) thin films were prepared on an Ir(100) single crystal.[26] The atomic structure of both cobalt oxide surfaces was previously established by STM and LEED I-V analysis.[24] The corresponding structures are shown in Scheme 2. Briefly, the Co_3O_4(111) surface is terminated by Co^{2+} ions in a hexagonal arrangement with a Co^{2+}–Co^{2+} distance of 5.7 Å. The CoO(100) surface is terminated both by Co^{2+} and O^{2-} ions in a quadratic unit cell. The Co^{2+}–Co^{2+} distance in this structure is 3.0 Å.

In the IL deposition studies, two types of experiments were performed. First, the coverage dependent adsorption behavior was investigated by time-resolved measurements in which IR spectra were recorded during deposition of the IL under isothermal conditions. These experiments provide information on the adsorption process, the interaction mechanism and the adsorption energy. Secondly, temperature-programmed measurements were performed, which provide information on the thermal stability of adsorbed states and the desorption temperature.

Previously, we have analyzed the IR spectrum of [BMIM][NTf_2] in detail based on the results of density functional calculations.[11] Following this work, we have summarized the peak positions and the peak assignments in Table 1. Briefly, the bands at 1062, 1110, 1216 and 1360 cm^{-1} are assigned to the symmetric CF stretching mode, $\nu(CF_3)_{sym}$, the symmetric SO_2 stretching mode, $\nu(SO_2)_{sym}$, the antisymmetric CF stretching mode, $\nu(CF_3)_{asym}$, and the antisymmetric SO stretching mode, $\nu(SO_2)_{asym}$, respectively.[11] Another region is the one above 1400 cm^{-1}. Here, several bands of the cations appear. For the non-functionalized [BMIM][NTf_2] these bands are comparable weak. The most prominent feature is the one at 1575 cm^{-1} which originates from the a CN/CC stretching mode in the aromatic ring, $\nu(C{=}N/C{=}C)_{ring}$. Naturally, this band is polarized par-

Table 1. Band positions and assignments for the three ILs used in this work after deposition onto $Co_3O_4(111)$ at 200 K.

IL/$Co_3O_4(111)$	Peak position [cm^{-1}] Sub-monolayer	Multilayer	Assignment
[BMIM][NTf_2]	1062, 1216, 1360	1062, 1216, 1360	$\nu(CF_3)_{sym}$, $\nu(CF_3)_{asym}$, $\nu(SO_2)_{asym}$
	1110	1140	$\nu(SO_2)_{sym}$
	1465	1465	$(CH_2)_{scissor}$
		1575	$\nu(C{=}N,C{=}C)_{ring}$
[MBMIM][NTf_2]	1062, 1216, 1360	1062, 1216, 1360	$\nu(CF_3)_{sym}$, $\nu(CF_3)_{asym}$, $\nu(SO_2)_{asym}$
	1110	1140	$\nu(SO_2)_{sym}$
	1465	1465	$(CH_2)_{scissor}$
	1685	1685	$\nu(C{=}O)_{surf}$
		1575, 1735	$\nu(C{=}N,C{=}C)_{ring}$, $\nu(C{=}O)_{ester}$
[IPBMIM][NTf_2]	1062, 1216, 1360	1062, 1216, 1360	$\nu(CF_3)_{sym}$, $\nu(CF_3)_{asym}$, $\nu(SO_2)_{asym}$
	1110	1140	$\nu(SO_2)_{sym}$
	1465	1465	$(CH_2)_{scissor}$
	1680	1680	$\nu(C{=}O)_{surf}$
		1575, 1728	$\nu(C{=}N,C{=}C)_{ring}$, $\nu(C{=}O)_{ester}$

allel to the imidazolium ring. A second broad feature centered at 1465 cm^{-1} is mostly due to the CH_2 deformation mode from the alkyl side chain of the cation. For the two functionalized ILs [MBMIM][NTf_2] and [IPBMIM][NTf_2] strong additional bands appear from the ester group at around 1700 cm^{-1}.

2.1. Adsorption of [BMIM][NTf_2], [MBMIM][NTf_2], and [IPBMIM][NTf_2] on $Co_3O_4(111)$ at 200 K

In the first step, isothermal adsorption experiment were performed for [MBMIM][NTf_2], [IPBMIM][NTf_2] and [BMIM][NTf_2] on $Co_3O_4(111)$ at 200 K. Each IL was deposited at a rate of approximately 0.05 ML per minute for a total deposition time of at least 60 mins. Here, we define the monolayer as the film thickness up to which the cations and anions interact with the surface. This interaction is monitored by the cation band at 1680 cm^{-1} and the anion bands at 1140 and 1216 cm^{-1} as will be described below. Above the monolayer, the IL adsorbs in the multilayer where there is no direct contact with the oxide. The corresponding IR spectra recorded during deposition are shown in Figure 1.

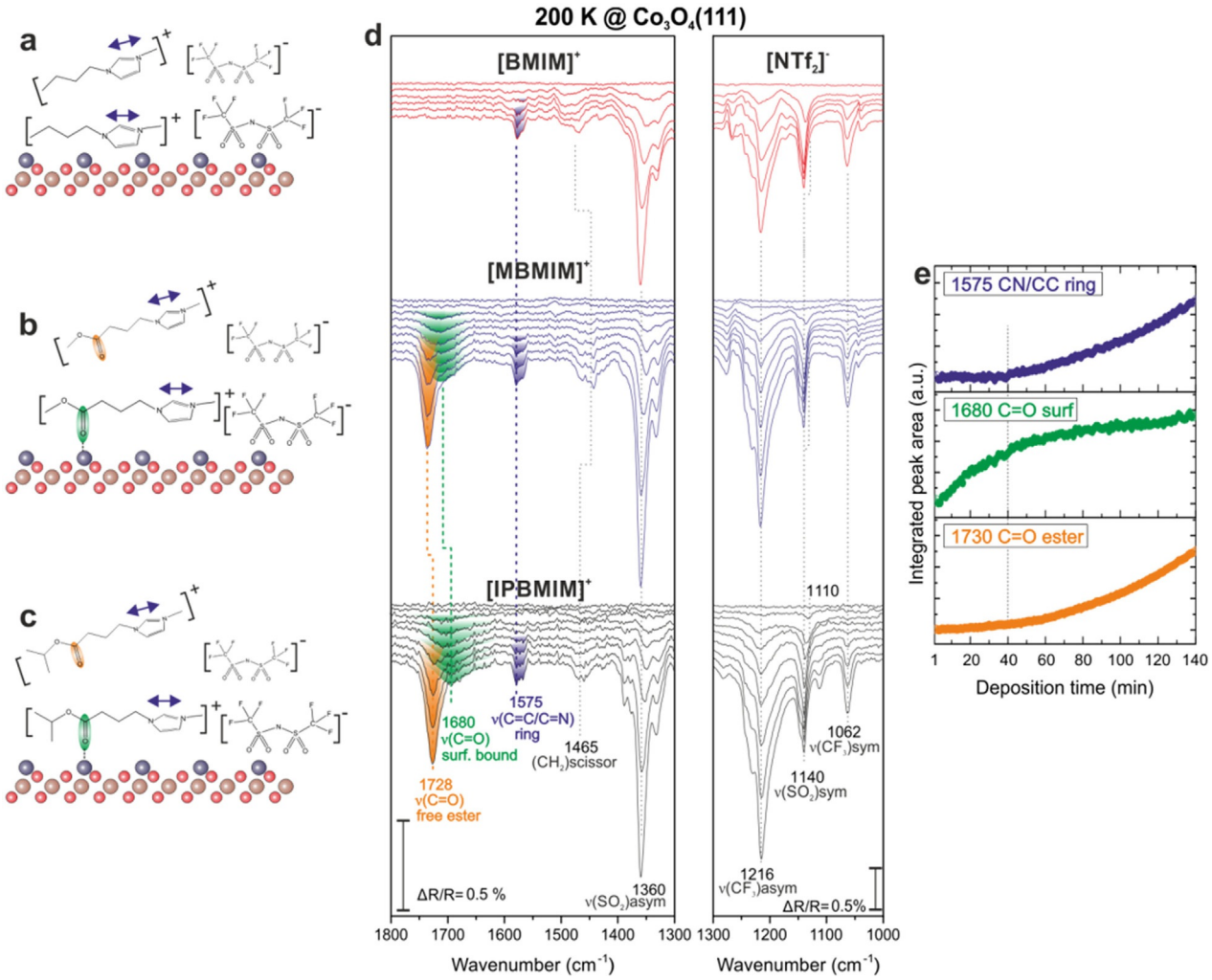

Figure 1. a–c) Schematic representation of surface contacting ILs on $Co_3O_4(111)$. d) Time resolved IRAS of [BMIM], [MBMIM] and [IPBMIM][NTf_2] adsorbing on $Co_3O_4(111)$ at 200 K. e) Integrated peak area of selected peaks plotted as a function of deposition time in the case of [IPBMIM][NTf_2] on $Co_3O_4(111)$ at 200 K.

At a substrate temperature of 200 K, adsorbed IL layers do not evaporate and, therefore, multilayers of all ILs can be accumulated. The corresponding spectra are displayed in Figure 1 d. For all three ILs, the most intense bands in the mid IR region can be grouped in two spectral regions. In the region from 1000 to 1400 cm^{-1}, several intense intensive peaks are observed, which mostly arise from the $[NTf_2]^-$ ion. The second important region is the one above 1400 cm^{-1}. Here, several bands of the cations appear. We first focus on the initial stages of deposition, where the IL is in direct contact with the cobalt oxide surface. In this region, we expect spectral changes for the characteristic modes of those molecular parts which directly interact with the surface. In addition, changes of the relative intensity of specific modes may occur which indicate preferential orientation of the ions. These intensity changes arise from the metal surface selection rule (MSSR), which states that only the perpendicular part of the dynamic dipole moment contributes to absorption in IRAS.[27] Note that the MSSR also holds for thin oxide films on metallic substrates, such as in the present system.

Inspecting the spectra for $[BMIM][NTf_2]$ in the monolayer region, we observe all characteristic bands which are also observed in the multilayer (see Figure 1 d, top). In addition to the anion bands at 1062, 1110, 1216 and 1360 cm^{-1}, we observe weak peaks at 1450 and 1570 cm^{-1} which indicate the presence of the cation. We conclude that $[BMIM][NTf_2]$ adsorbs molecularly on $Co_3O_4(111)$, similarly as was observed on other oxide surfaces before.[11] However, characteristic changes of the relative band intensities are observed between the monolayer and the multilayer region. Specifically, we find that the relative intensity of the $\nu(SO_2)_{sym}$ band at 1140 cm^{-1} and the $\nu(CF_3)_{asym}$ at 1216 cm^{-1} increases with decreasing coverage. In addition, the $\nu(SO_2)_{asym}$ at 1360 cm^{-1} changes its shape with decreasing coverages and transforms into a doublet at 1350 and 1330 cm^{-1}. Both effects have been observed previously for $[BMIM][NTf_2]$ on Al_2O_3. The spectral changes are characteristic for a $[NTf_2]^-$ ion which adopts a *cis*-conformation and interacts with the surface via the SO_2 groups.[11] We conclude that the adsorption behavior of $[NTf_2]^-$ on $Co_3O_4(111)$ is very similar in the sub-monolayer region. The proposed adsorption geometry is schematically depicted in Figure 1 a–c. Noteworthy, the relative changes in intensity are less pronounced for the functionalized ILs $[MBMIM][NTf_2]$ and $[IPBMIM][NTf_2]$ indicating that the orientation of the anion is less defined. A possible explanation for this effect is an enhanced interaction of the cation with the surface, which might interfere with the adsorption of the anion and leads to a less well-defined adsorption geometry.

Indeed, the spectra of the functionalized cations show clear indication for specific interactions between the functional group at the cation and the Co_3O_4 surface. The corresponding spectra for $[MBMIM][NTf_2]$ and $[IPBMIM][NTf_2]$ are displayed in Figure 1 d (middle and lower panel). Strong bands appear for the functionalized ILs around 1700 cm^{-1}, which arise from the ν(C=O) mode from the ester group in the cation. Interestingly, the spectral appearance of these bands changes drastically as a function of coverage. For the $[MBMIM][NTf_2]$, a broad band appears at low coverage at 1685 cm^{-1}, whereas in the multilayer region this band saturates and an additional sharp band grows a 1735 cm^{-1}. For $[IPBMIM][NTf_2]$ a very similar behavior is found (broad monolayer feature at 1680, sharp multilayer band at and 1728 cm^{-1}). The development of the peak intensities of the bands at 1680 and 1730 cm^{-1} as well as the $\nu(C{=}N/C{=}C)_{ring}$ mode at 1575 cm^{-1} is presented in Figure 1 e as a function of deposition time. We clearly observe that the band at 1680 cm^{-1} saturates after approximately 40 minutes while the other bands start to increase at this point in time.

Based on the above observation we attribute the band at 1680 cm^{-1} to the ν(C=O) mode of an ester group which is interacting with the $Co_3O_4(111)$ surface, presumable with the surface Co^{2+} ions. However, the red-shift is moderate and, clearly, the C=O bond remains intact upon interaction with the ester group. In the multilayer, no specific surface interaction is possible and we observe the regular ν(C=O) band of the free ester group at 1730 cm^{-1}. The absence of $\nu(C{=}N/C{=}C)_{ring}$ peak at 1575 cm^{-1} in the sub-monolayer region suggests that the imidazolium ring of the cation is lying flat on the surface, at least at low coverage. Similar adsorption structures have been suggested previously for other imidazolium-based ILs on metals.[28] The authors suggested that in the monolayer region anion and cation co-adsorb on the surface, forming a checkerboard-like pattern.

In the multilayer region, the intensity ratios observed in the IR spectra rapidly approached the bulk ratio. We conclude that preferential orientation is lost within the first IL monolayers. The corresponding interaction mechanisms and orientation of the cation in the sub-monolayer region are schematically represented in Figure 1 a–c.

2.2. Desorption of $[BMIM][NTf_2]$, $[MBMIM][NTf_2]$, and $[IPBMIM][NTf_2]$ from $Co_3O_4(111)$

In the next set of experiments, we investigated the thermal behavior of the multilayer IL films onto $Co_3O_4(111)$ in the temperature range from 200 to 573 K. To this aim, we performed temperature-programmed IR spectroscopy, that is, the sample was heated at a rate of 2 K min^{-1} while IR spectra were recorded continuously. As a IR background, we used the clean $Co_3O_4(111)$ surface. The recorded TP-IRAS data for $[BMIM][NTf_2]$, $[MBMIM][NTf_2]$, and $[IPBMIM][NTf_2]$ on $Co_3O_4(111)$ are displayed in form of contour plots in Figure 2.

In the IR data of $[BMIM][NTf_2]$ in Figure 2 a, we can identify three temperature regions. In the first region from 200 K to 360 K, no major changes can be observed in the IR spectra. All bands correspond to those discussed above for the $[BMIM][NTf_2]$ multilayer (see Section 3.1). At around 360 K, the multilayer IRAS peaks disappear and only some indications for very weak bands can be observed thereafter. The temperature of 360 K is very close to the multilayer desorption temperature for $[BMIM][NTf_2]$ observed in previous studies.[11,29] Therefore, we attribute the spectral changes at 360 K to desorption of the $[BMIM][NTf_2]$ multilayer. The second region is from 360 to 460 K, where only some weak peaks are visible. The most prominent feature is the one at 1140 cm^{-1} which we assign to the $\nu(SO_2)_{sym}$ mode of the $[NTf_2]^-$. The presence of the signals

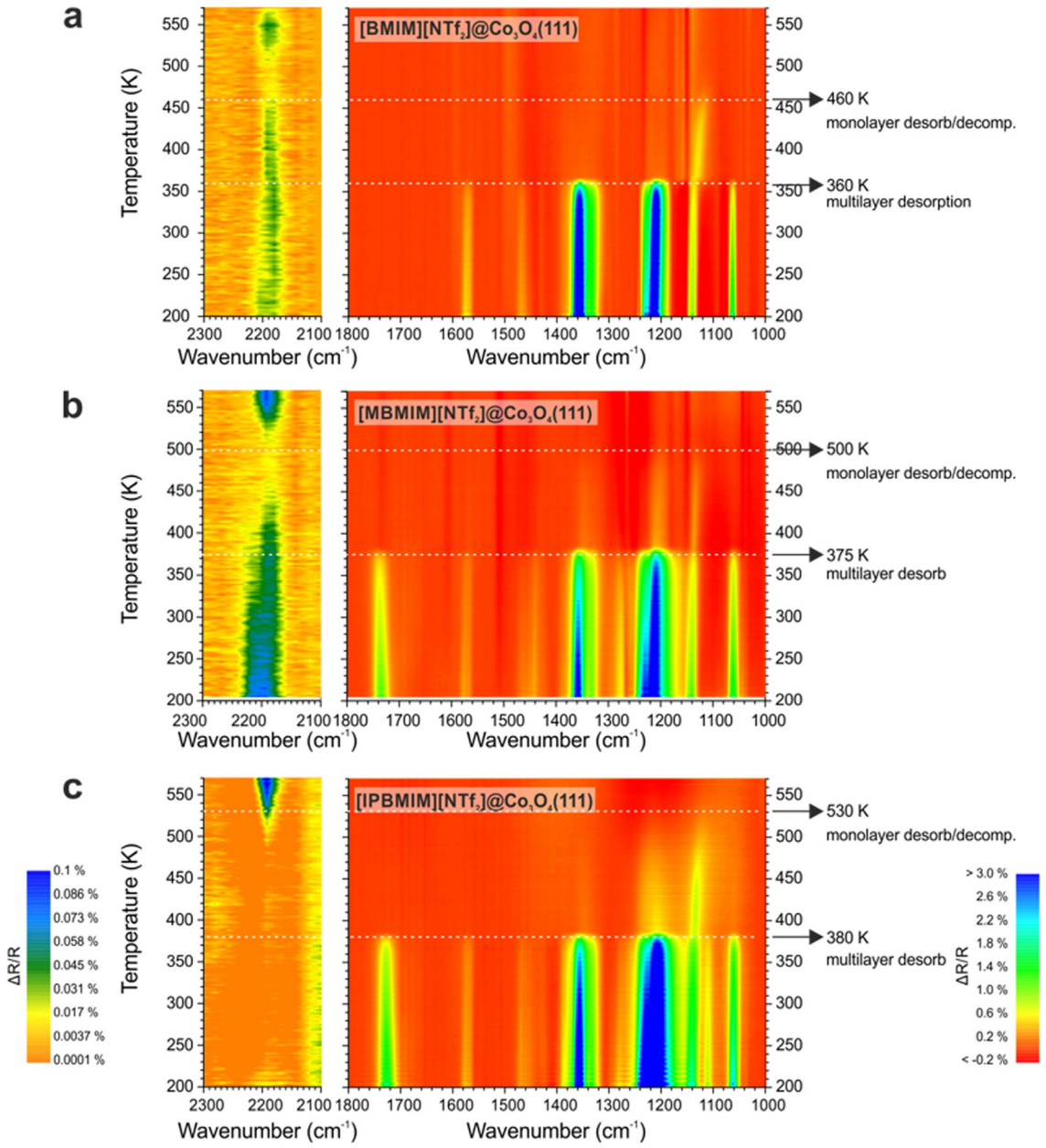

Figure 2. TP IRAS of a) [BMIM][NTf_2], b) [MBMIM][NTf_2], and c) [IPBMIM][NTf_2] thin films on Co_3O_4(111) surface. The IRAS peak intensity is represented in color as indicated by the color bars. The same color in the map indicates the same IRAS absorption intensity ($\Delta R/R$). For clarity, the spectral region between 2100 and 2300 cm^{-1} is colored with different color scale.

indicates that strongly bound species reside on the surface after multilayer desorption. Noteworthy, the $\nu(SO_2)_{sym}$ band is also the dominating feature in the adsorption experiments at low coverage (see Section 3.1). The high intensity is the result of the well-defined molecular orientation which the $[NTf_2]^-$ adopts in the first monolayer. In the TP-IRAS experiments the band gradually red-shifts from 1140 cm^{-1} to 1110 cm^{-1}. This behavior is the exact reverse of what is observed in the adsorption process. Such coverage dependent blue-shifts are often observed in IRAS and typically arise from dipole-dipole interactions.[27] Unfortunately, most other bands of the IL, in particular those of the cation, cannot be identified in the TR-IRAS spectra because of their low intensity. Therefore, we cannot provide clear evidence that the IL remains intact over the full range of temperature of region 2 (360 to 460 K). The slow decrease in intensity around 460 K may suggest, however, that the IL at least partially decomposes in this temperature range. At temperatures above 460 K (region 3), no bands at all can be observed in the IRAS spectra. A relatively weak band at around 2200 cm^{-1} can be identified which remains present up to high annealing temperatures on Co_3O_4(111). A decrease in intensity of this band could be observed when monolayer IL decomposes at 460 K. However, it quickly regains its original intensity when surface temperature is above 500 K. We tentatively assign this band to the CN bond in an isocyanide species. Most likely a small portion of the IL decomposes at low

temperature on defect sites to form isocyanide that adsorb strongly on the surface. Upon decomposition of the surface contacted IL, this band decreases in intensity, possibly due to orientation effects induced by IL decomposition. Thermal decomposition above 500 K leads to a further increase of the surface bound isocyanide fragments as indicated by the increase in band intensity at 2200 cm^{-1}.

The TP IRAS spectra of the ester-functionalized ILs [MBMIM][NTf_2] and [IPBMIM][NTf_2] are shown in Figure 2b and 2c, respectively. Their spectral behavior as a function temperature is very similar to that of [BMIM][NTf_2]. Again, we can divide the temperature range into three phases: multilayer desorption, monolayer desorption (possibly with partial decomposition) and desorption of all IR species. For [MBMIM][NTf_2], multilayer desorption takes place at around 380 K while desorption of the species from the monolayer occurs around 500 K. For [IPBMIM][NTf_2], multilayer desorption is observed at 380 K while the IR-active species from the monolayer disappear around 530 K. Overall, it can be summarized that the multilayer desorption temperature show the relation: T_m[IPBMIM] (380 ± 5 K) = T_m[MBMIM] (375 K ± 5 K) > T_m[BMIM] (360 K ± 5 K), whereas desorption of the surface species in the monolayer are observed at T_s[IPBMIM] (530 ± 30 K) > T_s[MBMIM] (500 ± 30 K) > T_s[BMIM] (460 ± 30 K). The higher multilayer desorption temperature of [IPBMIM] and [MBMIM][NTf_2] compared to the non-functionalized [BMIM][NTf_2] is due to the stronger intermolecular interactions through the polar ester group and larger van-der-Waals interactions. The similar multilayer desorption temperature of [IPBMIM] and [MBMIM][NTf_2] indicates that the main contribution to the intermolecular interactions originates from the ester group and not from the van-der-Waals interaction. The isocyanide band at 2200 cm^{-1} can also be found for the ester-functionalized ILs on the Co_3O_4(111) surface. For [MBMIM][NTf_2], the 2200 cm^{-1} band behaves similarly to the one formed from [BMIM][NTf_2]. However, for [IPBMIM][NTf_2] the isocyanide species is observed at high temperature only. This indicates that [IPBMIM][NTf_2] is somewhat more stable towards decomposition at surface defects.

2.3. Adsorption of [MBMIM][NTf_2] and [IPBMIM][NTf_2] on Co_3O_4(111) at 300 and 400 K

In a next set of experiments, we deposited the ester functionalized ILs [MBMIM] and [IPBMIM][NTf_2] onto Co_3O_4(111) surface at 300 and 400 K. The corresponding time-resolved IRAS spectra are shown in Figure 3 and 4, respectively. Again the reference spectrum was taken before IL deposition and the IR spectra were taken during the deposition process.

At 300 K, the IRAS data of [MBMIM][NTf_2] and [IPBMIM][NTf_2] are nearly identical to those at 200 K. We identify all characteristic features of the $[NTf_2]^-$ ion in the spectra. Presence of the $[MBMIM]^+$ or $[IPBMIM]^+$ ion is indicated by the characteristic $\nu(C{=}N/C{=}C)_{ring}$ stretching mode of the imidazolium ring at 1575 cm^{-1}. Again, a strong broadening and red-shift of the $\nu(C{=}O)$ band to 1680 cm^{-1} indicates the interaction of the ester group with the surface in the first monolayer. Beyond the monolayer, the characteristic band of the free ester group appears at 1728 cm^{-1} showing the growth of a non-specifically adsorbed multilayer. The preferential orientation of the $[NTf_2]^-$ ion is indicated by the large intensity of the $\nu(SO_2)_{sym}$ band which shows that anion adsorbs on the surface via the SO_2 groups (see Section 3.1). We conclude that, similarly to the situation at 200 K, both the anion and the cation directly co-adsorb on the Co_3O_4 surface via specific interaction mechanisms. After completion of the first monolayer, we observe the growth of the IL multilayer. Spectroscopically, we can identify the multilayer by the appearance of bands which do not show the characteristic peak shifts and intensity changes of the specifically adsorbed monolayer. We conclude that the preferential molecular orientation is rapidly lost, once the multilayer is formed.

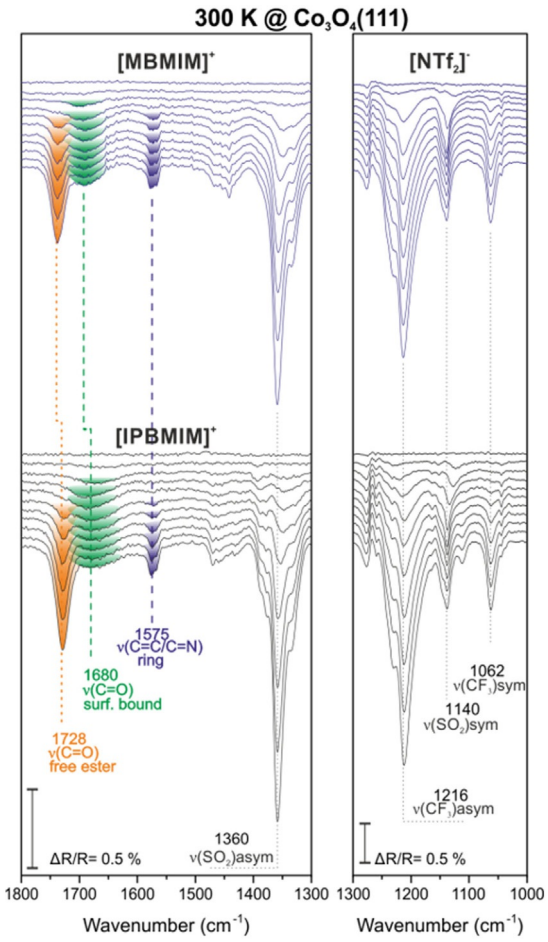

Figure 3. Time-resolved IRAS of [MBMIM][NTf_2] and [IPBMIM][NTf_2] on Co_3O_4(111) at 300 K.

Turning to the IL deposition experiment at 400 K (Figure 4), we observe that the IR bands saturate after appearance of the monolayer features and no multilayer bands are formed. This behavior is expected as we have shown in the TP-IRAS experiment that the [MBMIM][NTf_2] and [IPBMIM][NTf_2] multilayers desorb at 380 K. Noteworthy, the features observed at 400 K are nearly identical to the monolayer bands observed for deposition of small amounts of ILs at 300 K. The only difference is seen in the CN/CC band at 1575 cm^{-1} which is more promi-

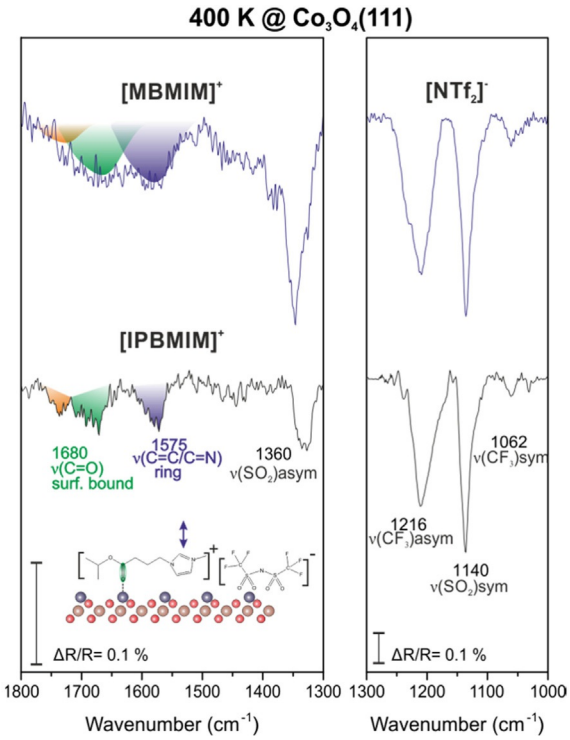

Figure 4. Sub-monolayer IRAS of $[MBMIM][NTf_2]$ and $[IPBMIM][NTf_2]$ on $Co_3O_4(111)$ at 400 K.

nent at 400 K indicating a more upstanding orientation of the imidazolium ring in the cations. Clearly, we identify the characteristic bands of the $[NTf_2]^-$ ion at 1062 cm^{-1} ($\nu(CF_3)_{sym}$), 1140 cm^{-1} ($\nu(SO_2)_{sym}$), 1216 cm^{-1} ($\nu(CF_3)_{asym}$) and 1360 cm^{-1} ($\nu(SO_2)_{asym}$). The intensity ratio of the $\nu(SO_2)_{sym}$ and the $\nu(CF_3)_{sym}$ bands is similar to that found in the sub-monolayer at 200 and 300 K, indicating that the $[NTf_2]^-$ ion is again oriented with the SO_2 group pointing towards the surface.

2.4. Adsorption and Desorption of $[BMIM][NTf_2]$ and $[IPBMIM][NTf_2]$ on CoO(100)

The isothermal adsorption experiments with the ester-functionalized ILs show that functionalization with the ester group can be utilized to introduce a specific interaction mechanism between cation of the IL and the surface. The findings suggest the interaction occurs by chemisorption of the carbonyl function of the ester group to a Co^{2+} ion of the $Co_3O_4(111)$ surface. Here, the two ester-functionalized ILs, [MBMIM] and [IPBMIM] $[NTf_2]$, show very similar behavior.

In the next step, we investigated whether the surface structure of the cobalt oxide has an effect on the interaction with functionalized and non-functionalized ILs. To this end, we prepared CoO(100) films on Ir(100) and probed their interaction with $[BMIM][NTf_2]$ and $[IPBMIM][NTf_2]$. In contrast to $Co_3O_4(111)$, the CoO(100) surface is terminated by both Co^{2+} and O^{2-} ions, with the Co^{2+}–Co^{2+} distance (3.0 Å) being much smaller than on $Co_3O_4(111)$ (5.7 Å). The IR data recorded for the isothermal adsorption experiments for $[IPBMIM][NTf_2]$ and $[BMIM][NTf_2]$ on CoO(100) are displayed in Figure 5 and 6, respectively. Both ILs were deposited at temperatures below (300 K) and above (400 K) the multilayer desorption temperature.

For the $[IPBMIM][NTf_2]$ at 300 K, we observed a behavior that is very similar to the one observed for adsorption on $Co_3O_4(111)$. Starting with the $[NTf_2]^-$ ion, we can identify all characteristic bands and also observe the changes in relative band intensities which indicate the adsorption of the $[NTf_2]^-$ ion via the SO_2 groups on the oxide surface. The presence of the cation is indicated by the $\nu(C{=}N/C{=}C)_{ring}$ stretching mode of the imidazolium ring at 1575 cm^{-1} and the $\nu(C{=}O)$ of the ester group. Similar as for $Co_3O_4(111)$, the C=O bond is broadened and red-shifted to 1680 cm^{-1} in the monolayer region indicating interaction of the ester group with the Co^{2+} ions in the CoO(100), before free ester groups ($\nu(C{=}O)$ at 1728 cm^{-1}) are observed in the multilayer regime.

A surprisingly different behavior was found, if $[IPBMIM][NTf_2]$ was deposited at 400 K, on which we reported recently in a short communication.[22] Here we present additional data at 300 and 375 K to discuss the behavior in greater detail (see Figure 5). In the anion region, we observe all characteristic bands of the $[NTf_2]^-$ ion (1062 cm^{-1} ($\nu(CF_3)_{sym}$), 1140 cm^{-1} ($\nu(SO_2)_{sym}$), 1216 cm^{-1} ($\nu(CF_3)_{asym}$), 1360 cm^{-1} ($\nu(SO_2)_{asym}$)) indicating that the anion is intact and adsorbs on the surface with the characteristic orientation discussed before (see Figure 5 and discussion above). Dramatic changes are observed, however, in the spectral region of the cation. We find that the characteristic $\nu(C{=}O)$ stretching band of the ester group (1680 cm^{-1} for the adsorbed and 1728 cm^{-1} for the free ester) is nearly absent and, instead, a new band appears at 1412 cm^{-1}. Previously, we studied the adsorption of various carboxylic acids on the same cobalt oxide film.[21b,30] Typically, these compounds adsorb by formation of a bridging surface carboxylate, which is characterized by the dominant bands of the symmetric stretching mode, $\nu_s(OCO)$, of a bridging surface carboxylate at around 1420 cm^{-1}. Note that the antisymmetric stretching mode, $\nu_{as}(OCO)$, at around 1540 cm^{-1} is not observed because of the MSSR. Accordingly, we attribute the new band at 1412 cm^{-1} to a surface carboxylate which is formed by cleavage of the ester group in the $[IPBMIM]^+$ ion by reaction with the surface. We suggest that in this reaction the isopropyl group is split off and leaves the surface by formation of a volatile fragment, such as for example, propene or acetone. This reaction leaves behind an imidazolium species anchored to the surface by a carboxylate group. The presence of the imidazolium ring in the surface-anchored fragment is evidenced by the characteristic $\nu(C{=}N/C{=}C)_{ring}$ stretching mode of the imidazolium ring at 1575 cm^{-1}.

In a reference experiment, we investigated the adsorption of the non-functionalized $[BMIM][NTf_2]$ on CoO(100) under identical conditions. The corresponding IR data is displayed in Figure 6. At 300 K, we observe the formation of IL multilayers. Both in the anion and in the cation region, we observe all characteristic bands (see Section 5.1) which allows us to conclude that the $[BMIM][NTf_2]$ adsorbs molecularly on CoO(100). No indication for specific chemical interactions are observed apart from the preferential orientation of the $[NTf_2]^-$ ion in the first monolayer, which is the same as observed in all other sys-

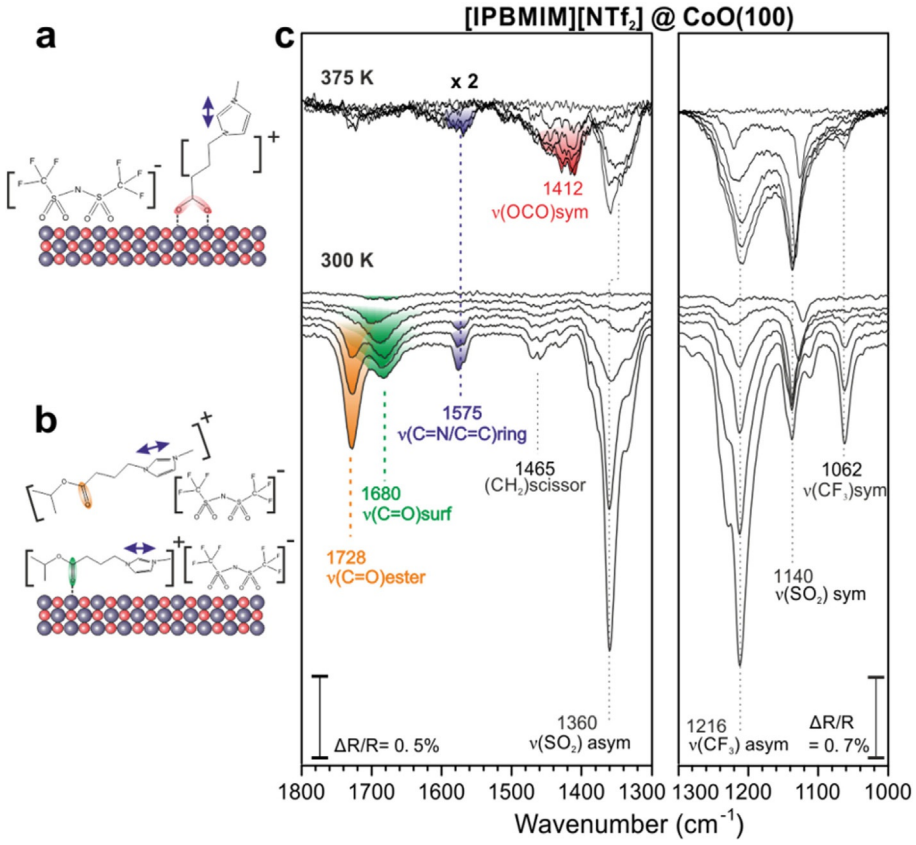

Figure 5. Schematic representation of [IPBMIM][NTf_2] on CoO(100) at a) 375 K and b) 300 K. c) Time-resolved IRAS of [IPBMIM][NTf_2] on CoO(100) at 375 and 300 K.

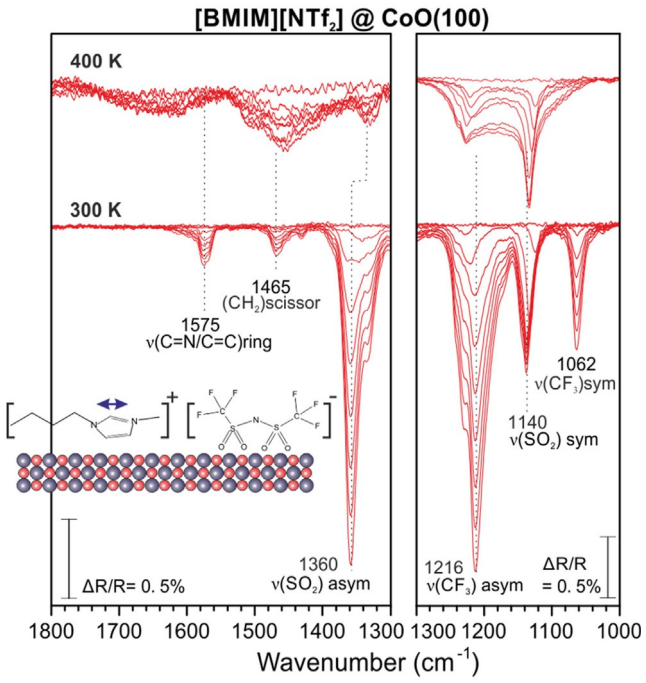

Figure 6. Time-resolved IRAS of [BMIM][NTf_2] on CoO(100) at 300 and 400 K. Inset is a schematic representation of [BMIM][NTf_2] on CoO(100) at 300 K.

tems discussed above. For adsorption at 400 K, the spectra are dominated by a number of broad bands which are characteristic for the $[NTf_2]^-$ ion. However, no clear evidence was found for the presence of the $\nu(C{=}N/C{=}C)_{ring}$ mode of the imidazolium group. This implies that either the imidazolium group of the $[BMIM]^+$ lies flat on the surface or that the IL decomposes partially and the cation desorbs from the surface by formation of volatile products. The large width of the bands may suggest that at least a part of the IL indeed undergoes decomposition.

Finally, we studied the thermal behavior of [BMIM][NTf_2] and [IPBMIM][NTf_2] multilayers on CoO(100) in an experiment similar to the one shown in Figure 2 for Co_3O_4(111). As shown in Figure 7, desorption of the IL multilayer is observed at 360 K for [BMIM][NTf_2] and at 380 K for [IPBMIM][NTf_2]. Not surprisingly, these temperatures are identical to those observed on Co_3O_4(111).

For both ILs, weak features reside above the monolayer desorption temperature. For the non-functionalized [BMIM][NTf_2] the most prominent peak is the $\nu(SO_2)_{sym}$ band at 1140 cm^{-1} which only gradually decreases in intensity with increasing temperature and can still be observed at temperatures above 550 K. The high thermal stability suggests that the IL indeed decomposes and $[NTf_2]^-$ derived fragments reside which decompose only slowly at high temperature. Recently, we observed a similar behavior for a very similar IL on a CeO_2 sur-

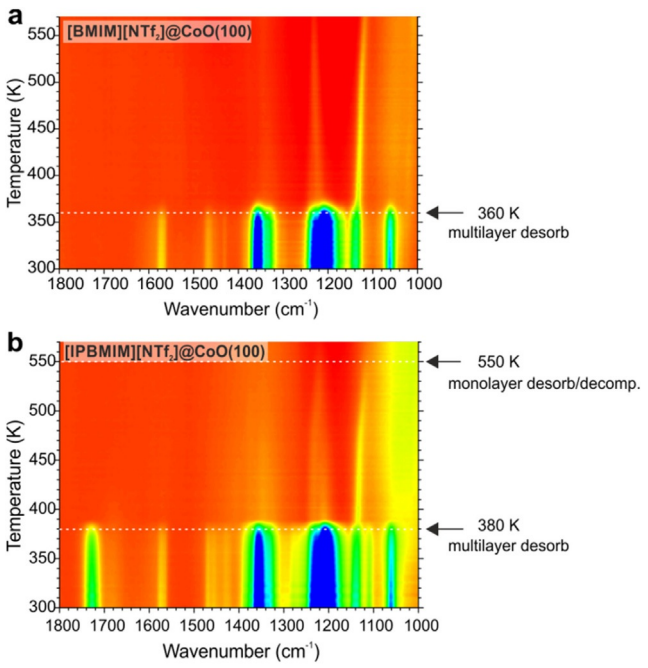

Figure 7. TP IRAS of a) [BMIM][NTf_2] and b) [IPBMIM][NTf_2] thin film on a CoO(100) surface.

face.[12,31] A similar behavior is also found for [IPBMIM][NTf_2] above the multilayer desorption temperature. Here, the most striking observation is that the new carboxylate band ν_s(OCO) at 1412 cm^{-1} which is indicative of the surface-bound imidazolium ion is rather weak. This observation is in-line with the idea that the scission of the ester bond and the formation of the surface carboxylate is an activated process which occurs at elevated temperatures only. In the TP-IRAS experiment, desorption competes with scission of the ester bond and, consequently, the surface coverages of the anchored species are lower than those formed during extended exposure to [IPBMIM][NTf_2] at elevated temperature.

Summarizing the above findings, we find that for all ILs and both cobalt oxide surfaces, the $[NTf_2]^-$ ion shows a similar behavior upon adsorption. The species adsorbs molecularly on all surfaces at temperatures up to 400 K, adopts a *cis*-conformation and interacts with the surface via its SO_2 groups. The surface interaction of the imidazolium ion can be controlled by functionalization, that is, introduction of an ester group onto one of the alkyl side chains. On both, the Co_3O_4(111) and the CoO(100) surface, the ester group can bind weakly to the surface via interaction of the C=O with the Co^{2+} ions. While the latter interaction mechanism is the only one observed on Co_3O_4(111), a second reaction channel is found for [IPBMIM][NTf_2] on CoO(100). Here, a C–O bond of the ester can be cleaved, leading to the formation of an imidazolium species, which is anchored to the surface by formation of a surface carboxylate. The key difference between the CoO(100) and the Co_3O_4(111) surface is the distance between the surface Co^{2+} ions.[22] The smaller Co^{2+}–Co^{2+} distance of 3.0 Å on CoO(100) permits formation of a bridging carboxylate, whereas this adsorption geometry is not possible on the Co_3O_4(111) surface with a Co^{2+}–Co^{2+} distance of 5.7 Å. On the latter surface, a chelating carboxylate could be formed, which has a lower stability however.[32] As a consequence, we expect a larger driving force for carboxylate formation on CoO(100). We envisage that in future work such structure-dependent anchoring reactions could be utilized to prepare nanostructured IL-oxide interfaces.

3. Conclusions

We have studied the adsorption and reaction of three ILs, 3-butyl-1-methylimidazolium bis(trifluoromethyl-sulfonyl)imide ([BMIM][NTf_2]), 3-(4-methoxyl-4-oxobutyl)-1-methylimidazolium bis(trifluoromethyl-sulfonyl)imide ([MBMIM][NTf_2]) and 3-(4-isopropoxy-4-oxobutyl)-1-methylimidazolium bis(trifluoromethyl-sulfonyl) imide ([IPBMIM][NTf_2]) on two atomically-defined cobalt oxide surface, namely Co_3O_4(111) and CoO(100). All ILs were deposited by PVD method under UHV conditions. The Co_3O_4(111) and CoO(100) surfaces were prepared in form of thin films by reactive deposition of Co atoms in oxygen atmosphere on Ir(100). Adsorption, reaction, film growth were studied in situ by time-resolved and temperature-programmed IRAS. The main findings can be summarized as follows:

1) *Surface interaction of the $[NTf_2]^-$ ion:* On both cobalt oxide surfaces, all ILs physisorb at temperatures up to 300 K. The $[NTf_2]^-$ ion shows a preferential adsorption geometry and orientation in the first monolayer. It adopts a *cis*-conformation and interacts with the surface via the SO_2 groups. In the multilayer, the preferential orientation is rapidly lost.
2) *Surface interaction of the cations:* For all three ILs and at sub-monolayer coverage, the imidazolium ring in the cation is generally oriented parallel to the surface. For the ester-functionalized ILs [MBMIM][NTf_2] and [IPBMIM][NTf_2] the cation shows a characteristic interaction with both cobalt oxide surfaces. Here, the C=O group of the ester function binds weakly to a surface Co^{2+} ion. The ester group of the cation, however, remains intact in spite of this interaction with the surface.
3) *Multilayer and monolayer desorption:* For all three ILs, we determined the multilayer desorption temperatures T_{des} by temperature-programmed IRAS (heating rate 2 K min^{-1}): T_{des}(BMIM) = 360 ± 5 K; T_{des}(MBMIM) = 375 ± 5 K; T_{des}(IPBMIM) = 380 ± 5 K. After desorption of the multilayer, strongly adsorbed monolayer species reside on the surface. These species desorb and decompose over a broader temperature range from 450 to 550 K.
4) *Structure dependent surface reaction of [IPBMIM][NTf_2]:* Upon deposition of the ILs at temperatures slightly above the multilayer desorption temperature (400 K), more strongly adsorbed monolayers of molecularly adsorbed ILs are formed. An exception is [IPBMIM][NTf_2] deposited on CoO(100). Here, deposition at 400 K leads to cleavage of the ester bond in the $[IPBMIM]^+$ ion. This surface reaction yields an imidazolium species which is anchored to the surface via a bridging surface carboxylate. The surface reaction is structure sensitive and is not observed on Co_3O_4(111).

Acknowledgements

This project was financially supported by the Deutsche Forschungsgemeinschaft (DFG) within the Priority Program 1708 "Materials Synthesis near Room Temperature" and the Research Unit FOR 1878 "funCOS—Functional Molecular Structures on Complex Oxide Surfaces". Additional support is acknowledged from the Excellence Cluster "Engineering of Advanced Materials" and by the DFG within the DACH Project "COMCAT'. T.X. gratefully acknowledges a Ph.D. grant from the China Scholarship Council (CSC). In addition, we acknowledge travel support through the CONICET/ BAYLAT project "Cobalt based catalysts: finding structure–reactivity relationships".

Conflict of interest

The authors declare no conflict of interest.

Keywords: chemical anchoring · cobalt oxide · ionic liquids · IRAS · thermal stability

[1] P. Wasserscheid, A. Stark, in *Handbook of Green Chemistry—Green Solvents, Vol. 6* (Ed.: T. Anastas), Wiley-VCH, Weinheim, **2013**.
[2] a) H.-P. Steinrück, P. Wasserscheid, *Catal. Lett.* **2015**, *145*, 380 – 397; b) U. Kernchen, B. Etzold, W. Korth, A. Jess, *Chem. Eng. Technol.* **2007**, *30*, 985 – 994.
[3] W. Xu, C. A. Angell, *Science* **2003**, *302*, 422 – 425.
[4] S. R. Catarelli, S. J. Higgins, W. Schwarzacher, B.-W. Mao, J.-W. Yan, R. J. Nichols, *Langmuir* **2014**, *30*, 14329 – 14336.
[5] a) C. P. Mehnert, R. A. Cook, N. C. Dispenziere, M. Afeworki, *J. Am. Chem. Soc.* **2002**, *124*, 12932 – 12933; b) M. V. Fedorov, A. A. Kornyshev, *Chem. Rev.* **2014**, *114*, 2978 – 3036; c) D. R. MacFarlane, N. Tachikawa, M. Forsyth, J. M. Pringle, P. C. Howlett, G. D. Elliott, J. H. Davis, M. Watanabe, P. Simon, C. A. Angell, *Energy Environ. Sci.* **2014**, *7*, 232 – 250; d) A. Hagfeldt, G. Boschloo, L. Sun, L. Kloo, H. Pettersson, *Chem. Rev.* **2010**, *110*, 6595 – 6663; e) T. Sekitani, T. Someya, *Adv. Mater.* **2010**, *22*, 2228 – 2246; f) M. Armand, F. Endres, D. R. MacFarlane, H. Ohno, B. Scrosati, *Nat. Mater.* **2009**, *8*, 621 – 629.
[6] a) H. P. Steinrück, J. Libuda, P. Wasserscheid, T. Cremer, C. Kolbeck, M. Laurin, F. Maier, M. Sobota, P. S. Schulz, M. Stark, *Adv. Mater.* **2011**, *23*, 2571 – 2587; b) H.-P. Steinrück, *Surf. Sci.* **2010**, *604*, 481 – 484.
[7] M. Gorlov, L. Kloo, *Dalton Trans.* **2008**, 2655 – 2666.
[8] a) J. Wu, Z. Lan, J. Lin, M. Huang, Y. Huang, L. Fan, G. Luo, *Chem. Rev.* **2015**, *115*, 2136 – 2173; b) S. H. Kim, K. Hong, W. Xie, K. H. Lee, S. Zhang, T. P. Lodge, C. D. Frisbie, *Adv. Mater.* **2013**, *25*, 1822 – 1846.
[9] a) Y. Lauw, M. D. Horne, T. Rodopoulos, V. Lockett, B. Akgun, W. A. Hamilton, A. R. J. Nelson, *Langmuir* **2012**, *28*, 7374 – 7381; b) R. Hayes, N. Borisenko, M. K. Tam, P. C. Howlett, F. Endres, R. Atkin, *J. Phys. Chem. C* **2011**, *115*, 6855 – 6863; c) B. Uhl, M. Hekmatfar, F. Buchner, R. J. Behm, *Phys. Chem. Chem. Phys.* **2016**, *18*, 6618 – 6636; d) B. R. Lee, H. Choi, J. SunPark, H. J. Lee, S. O. Kim, J. Y. Kim, M. H. Song, *J. Mater. Chem.* **2011**, *21*, 2051 – 2053; e) M. Mezger, H. Schröder, H. Reichert, S. Schramm, J. S. Okasinski, S. Schöder, V. Honkimäki, M. Deutsch, B. M. Ocko, J. Ralston, M. Rohwerder, M. Stratmann, H. Dosch, *Science* **2008**, *322*, 424 – 428; f) A. K. Gupta, Y. L. Verma, R. K. Singh, S. Chandra, *J. Phys. Chem. C* **2014**, *118*, 1530 – 1539; g) S. Baldelli, *J. Phys. Chem. Lett.* **2013**, *4*, 244 – 252; h) M. Wagstaffe, M. J. Jackman, K. L. Syres, A. Generalov, A. G. Thomas, *ChemPhysChem* **2016**, *17*, 3430 – 3434.
[10] a) C. P. Mehnert, *Chem. Eur. J.* **2005**, *11*, 50 – 56; b) M. H. Valkenberg, C. deCastro, W. F. Holderich, *Green Chem.* **2002**, *4*, 88 – 93.
[11] M. Sobota, I. Nikiforidis, W. Hieringer, N. Paape, M. Happel, H. P. Steinrück, A. Görling, P. Wasserscheid, M. Laurin, J. Libuda, *Langmuir* **2010**, *26*, 7199 – 7207.
[12] S. Schernich, M. Laurin, Y. Lykhach, H.-P. Steinrück, N. Tsud, T. Skála, K. C. Prince, N. Taccardi, V. Matolín, P. Wasserscheid, J. Libuda, *J. Phys. Chem. Lett.* **2013**, *4*, 30 – 35.
[13] Y. G. Aronoff, B. Chen, G. Lu, C. Seto, J. Schwartz, S. L. Bernasek, *J. Am. Chem. Soc.* **1997**, *119*, 259 – 262.
[14] B. M. Silverman, K. A. Wieghaus, J. Schwartz, *Langmuir* **2005**, *21*, 225 – 228.
[15] a) M. Forster, M. S. Dyer, M. Persson, R. Raval, *J. Am. Chem. Soc.* **2009**, *131*, 10173 – 10181; b) M. Rodenstein, S. Zürcher, S. G. P. Tosatti, N. D. Spencer, *Langmuir* **2010**, *26*, 16211 – 16220; c) M. Urbani, M. Grätzel, M. K. Nazeeruddin, T. Torres, *Chem. Rev.* **2014**, *114*, 12330 – 12396.
[16] a) H. L. Ngo, K. LeCompte, L. Hargens, A. B. McEwen, *Thermochim. Acta* **2000**, *357 – 358*, 97 – 102; b) C. P. Fredlake, J. M. Crosthwaite, D. G. Hert, S. N. V. K. Aki, J. F. Brennecke, *J. Chem. Eng. Data* **2004**, *49*, 954 – 964.
[17] a) A. Deyko, T. Cremer, F. Rietzler, S. Perkin, L. Crowhurst, T. Welton, H.-P. Steinrück, F. Maier, *J. Phys. Chem. C* **2013**, *117*, 5101 – 5111; b) T. Cremer, M. Killian, J. M. Gottfried, N. Paape, P. Wasserscheid, F. Maier, H.-P. Steinrück, *ChemPhysChem* **2008**, *9*, 2185 – 2190.
[18] F. Jiao, H. Frei, *Angew. Chem. Int. Ed.* **2009**, *48*, 1841 – 1844; *Angew. Chem.* **2009**, *121*, 1873 – 1876.
[19] a) X. Deng, H. Tüysüz, *ACS Catal.* **2014**, *4*, 3701 – 3714; b) Y. Liang, Y. Li, H. Wang, J. Zhou, J. Wang, T. Regier, H. Dai, *Nat. Mater.* **2011**, *10*, 780 – 786.
[20] H. Yoshikawa, K. Hayashida, Y. Kozuka, A. Horiguchi, K. Awaga, S. Bandow, S. Iijima, *Appl. Phys. Lett.* **2004**, *85*, 5287 – 5289.
[21] a) T. Xu, S. Mohr, M. Amende, M. Laurin, T. Dopper, A. Görling, J. Libuda, *J. Phys. Chem. C* **2015**, *119*, 26968 – 26979; b) T. Xu, M. Schwarz, K. Werner, S. Mohr, M. Amende, J. Libuda, *Chem. Eur. J.* **2016**, *22*, 5384 – 5396; c) K. Werner, S. Mohr, M. Schwarz, T. Xu, M. Amende, T. Dopper, A. Görling, J. Libuda, *J Phys Chem. Lett.* **2016**, *7*, 555 – 560.
[22] T. Xu, T. Waehler, J. Vecchietti, A. Bonivardi, T. Bauer, J. Schwegler, P. S. Schulz, P. Wasserscheid, J. Libuda, *Angew. Chem. Int. Ed.* **2017**, *56*, 9072 – 9076; *Angew. Chem.* **2017**, *129*, 9200 – 9204.
[23] A. Desikusumastuti, T. Staudt, M. Happel, M. Laurin, J. Libuda, *J. Catal.* **2008**, *260*, 315 – 328.
[24] W. Meyer, K. Biedermann, M. Gubo, L. Hammer, K. Heinz, *J. Phys. Condens. Matter* **2008**, *20*, 265011.
[25] M. Gubo, C. Ebensperger, W. Meyer, L. Hammer, K. Heinz, F. Mittendorfer, J. Redinger, *Phys. Rev. Lett.* **2012**, *108*, 066101.
[26] K. Heinz, L. Hammer, *J. Phys. Condens. Matter* **2013**, *25*, 173001.
[27] F. Hoffmann, *Surf. Sci. Rep.* **1983**, *3*, 107.
[28] T. Cremer, L. Wibmer, S. K. Calderon, A. Deyko, F. Maier, H. P. Steinrück, *Phys. Chem. Chem. Phys.* **2012**, *14*, 5153 – 5163.
[29] M. Sobota, M. Schmid, M. Happel, M. Amende, F. Maier, H. P. Steinrück, N. Paape, P. Wasserscheid, M. Laurin, J. M. Gottfried, J. Libuda, *Phys. Chem. Chem. Phys.* **2010**, *12*, 10610 – 10621.
[30] M. Schwarz, S. Mohr, T. Xu, T. Döpper, C. Weiß, K. Civale, A. Hirsch, A. Görling, J. Libuda, *J. Phys. Chem. C* **2017**, *121*, 11508 – 11518.
[31] S. Schernich, M. Laurin, Y. Lykhach, N. Tsud, M. Sobota, T. Skála, K. C. Prince, N. Taccardi, V. Wagner, H.-P. Steinrück, V. Matolín, P. Wasserscheid, J. Libuda, *ChemPhysChem* **2013**, *14*, 3673 – 3677.
[32] T. Xu, M. Schwarz, K. Werner, S. Mohr, M. Amende, J. Libuda, *Phys. Chem. Chem. Phys.* **2016**, *18*, 10419-10427.

Manuscript received: July 28, 2017
Revised manuscript received: September 11, 2017
Accepted manuscript online: September 12, 2017
Version of record online: October 13, 2017